Assessment of Mean Apparent Propagator-Based Indices as Biomarkers of Axonal Remodeling after Stroke

Lorenza Brusini[1], Silvia Obertino[1], Mauro Zucchelli[1], Ilaria Boscolo Galazzo[2], Gunnar Krueger[3], Cristina Granziera[4], and Gloria Menegaz[1]

[1] Dept. of Computer Science, University of Verona, Italy
[2] Institute of Nuclear Medicine, University College of London, UK
[3] Siemens Healthcare USA, Boston, USA
[4] Dept. of Clinical Neuroscience, CHUV and University of Lausanne, Switzerland

Abstract. Recently, a robust mathematical formulation has been introduced for the closed-form analytical reconstruction of the signal and the Mean Apparent Propagator (MAP) in diffusion MRI. This is referred to as MAP-MRI or 3D-SHORE depending on the chosen reference frame. From the MAP, microstructural properties can be inferred by the derivation of indices that under certain circumstances allow the estimation of pores' geometry and local diffusivity, holding the potential of becoming the next generation of microstructural numerical biomarkers. In this work, we propose the assessment and validation of a subset of such indices that is RTAP, D, and PA for the quantitative analysis of axonal remodeling in the uninjured motor network after stroke. Diffusion Spectrum Imaging (DSI) was performed on ten patients and ten controls at different time points and the indices were derived and exploited for tract-based quantitative analysis. Our results provide quantitative evidence on the eligibility of the derived indices as microstructural biomarkers.

1 Introduction

Connectivity remodeling after stroke has been reported in both injured [1] and uninjured hemispheres [2,3]. Generalized Fractional Anisotropy (GFA) had previously been successfully exploited to provide evidence of plasticity in the uninjured motor network in stroke patients with motor deficits. Recently, a robust mathematical formulation has been introduced for the closed-form analytical reconstruction of the diffusion signal from which new micro structural indices could be analytically derived. This is referred to as Mean Apparent Propagator (MAP)-MRI and 3D Simple Harmonic Oscillator Based Reconstruction and Estimation (3D-SHORE), respectively, depending on the reference frame. The corresponding MAP, also known in literature as Ensemble Average Propagator (EAP) [4], can then be profitably exploited for deriving information about the ensemble average values of pores' geometry and local diffusivity [4] and hold the potential for eligibility as the next generation of microstructural biomarkers. In particular, an estimation of the axons' cross-sectional area and diameter

© Springer International Publishing Switzerland 2015
N. Navab et al. (Eds.): MICCAI 2015, Part I, LNCS 9349, pp. 199–206, 2015.
DOI: 10.1007/978-3-319-24553-9_25

can be derived analytically in white matter. In this work, we aimed at exploring whether the MAP-derived measures 1) could reveal contralesional structural changes along intracallosal connections after stroke; 2) correlate with the well established GFA index; and 3) jointly with clinical status allow to predict motor outcomes.

2 Materials and Methods

Ten stroke patients [6 males and 4 females (age: 60.3 ± 12.8 years, mean ± SD)] were enrolled in the study; the inclusion criteria, imaging protocol and post-processing were as in [2]. All patients underwent three DSI scans (TR/TE = 6600/138 msec, FOV = 212 × 212 mm, 34 slices, 2.2 × 2.2 × 3 mm resolution, 258 gradient directions, b_{max} = 8000 s/mm^2) within one week (*tp1*), one month (± one week, *tp2*), and six months (± fifteen days, *tp3*) after stroke. Orientation distribution functions were reconstructed using the Diffusion Toolkit (www.trackvis.org/dtk). Fiber-tracking was performed via a streamline algorithm (www.cmtk.org). Patients benefited of clinical assessment (NIHSS: National Institute of Health Stroke Scale), with the motor part (NIHSS motor) derived from items 2 to 7 and 10 (www.nihstrokescale.org/). Ten age and gender matched healthy controls were also included in the study (age: 56.1 ± 17.8 years, mean ± SD). Control group underwent two DSI scans one month apart (*tp1c* and *tp2c*). All subjects provided written informed consent and the Lausanne University Hospital review board approved the study protocol. To the best of our knowledge, this is the first attempt of using MAP-indices in patients, while *in-vivo* acquisition in healthy subjects were reported in [5].

2.1 Analytical Model for Signal Reconstruction

In this work, the orthonormal formulation of the 3D-SHORE model was chosen [6,7]. With respect to MAP, this formulation allows less degrees of freedom in the choice of the scale parameter but there is some evidence for improved capability in resolving complex structural micro-topologies [8]. The diffusion signal is modeled by using the Eigenfunctions of the SHORE as basis. After rotating the reference frame for diagonalizing the stiffness tensor, a separable solution can be obtained [4]

$$\Phi_{N_i}(\mathbf{A},\mathbf{q}) = \phi_{n_{x(i)}}(u_x,q_x)\phi_{n_{y(i)}}(u_y,q_y)\phi_{n_{z(i)}}(u_z,q_z) \quad (1)$$
$$\text{with} \begin{cases} \phi_n(u,q) = \frac{i^{-n}}{\sqrt{2^n n!}} e^{-2\pi^2 q^2 u^2} H_n(2\pi u q) \\ \mathbf{A} = \text{Diag}(u_x^2, u_y^2, u_z^2) \end{cases}$$

where $N_i = (n_{x(i)}, n_{y(i)}, n_{z(i)})$ is the basis order and H_n a Hermite polynomial. Diagonalization of the stiffness tensor is performed by tensor fitting $\mathbf{A}'$ ($\mathbf{A} = \mathbf{R}\mathbf{A}'\mathbf{R}^T$), where $\mathbf{R}$ consists of the tensor Eigenvectors. Separability enables the anisotropic scaling of the basis functions along the coordinate axes making the 3D basis particularly suited to anisotropic data. The 3D-SHORE

model is expressed in spherical coordinates. Separability holds the radial and angular coordinates which prevents the independent scaling of the basis functions along the main coordinate axes. Following the formulation in [9], the basis functions $\Phi_n(q\mathbf{u})$ can be written as

$$\Phi_n(q\mathbf{u}) = R_n(q)Y_n(\mathbf{u}) \tag{2}$$

where $R_n(q)$ models the radial part of the signal and $\{Y_n(\mathbf{u})\}$ are the real spherical harmonics of even order [10]. After a reordering of the terms, the signal model becomes

$$\mathbf{E}(q\mathbf{u}) = \sum_{l=0,even}^{N_{max}} \sum_{n=l}^{(N_{max}+l)/2} \sum_{m=-l}^{l} c_{nlm}\Phi_{nlm}(q\mathbf{u}) \tag{3}$$

$$\Phi_{nlm}(q\mathbf{u}) = \left[\frac{2(n-l)!}{\zeta^{3/2}\Gamma(n+3/2)}\right]^{1/2} \left(\frac{q^2}{\zeta}\right)^{l/2} \exp\left(\frac{-q^2}{2\zeta}\right) L_{n-l}^{l+1/2}\left(\frac{q^2}{\zeta}\right) Y_l^m(\mathbf{u})$$

where N_{max} is the maximal order in the truncated series and $\Phi_{nlm}(\mathbf{q})$ is the orthonormal 3D-SHORE basis, Γ is the Gamma function and ζ is an isotropic scaling parameter. The coefficients are determined by quadratic programming and positivity constraints are imposed to the MAP. The two formulations are equivalent for isotropic scaling.

Under such assumption, in this study we call MAP-based indices the measures derived from 3D-SHORE namely the Return to Axis Probability (RTAP) and Propagator anisotropy (PA). An estimate of the axon diameter (D) was inferred from RTAP as this provides an estimate of the exact statistical average of the cross-sectional area in white matter if some conditions are met [4] as $D = \sqrt{4\pi\ /RTAP}$. The MAP indices were assessed against GFA.

$$RTAP = \sum_{l=0,even}^{N_{max}} \sum_{n=l}^{(N_{max}+l)/2} \sum_{m=-l}^{l} c_{nlm} \left[\frac{\zeta^{1/2}\ 2^{l+3}\pi^2\ \Gamma(l/2+1)^2\ \Gamma(n+3/2)}{(n-l)!\ \Gamma(l+3/2)^2}\right]^{1/2} \times$$
$$\times\ {}_2F_1(l-n, l/2+1, l+3/2, 2)\ P_l(0)\ Y_l^m(\mathbf{u}^*)$$
$$PA = \sqrt{1 - \frac{\sum_{l=0}^{N_{max}/2+1} c_{l00}^2}{\sum_{l=0,even}^{N_{max}} \sum_{n=l}^{(N_{max}+l)/2} \sum_{m=-l}^{l} c_{nlm}^2}} \tag{4}$$

2.2 Tract-Based Quantitative Analysis

The primary motor area (M1), supplementary motor area (SMA), somatosensory cortex (SC) and thalamus (Thl) were considered in the analysis. GFA and MAP-indices were collected along intracallosal fiber bundles connecting those regions to the corpus callosum (CC) in the contralateral (non-lesioned) hemisphere. In particular, GFA, RTAP, D, and PA values were computed for each voxel and then averaged along each tract and among all tracts connecting the regions of interest to the CC.

2.3 Statistical Analysis

Reproducibility of mean GFA, RTAP, D, and PA values along motor tracts was assessed by evaluating statistical differences between *tp1c* and *tp2c* using a paired t-test ($p > 0.05$) after a Kolmogorov-Smirnov normality test. Percentage absolute changes in mean values between time points were evaluated for each index on both groups as

$$\begin{aligned} \Delta_{tp12c}(m) &= |(m_{tp2c} - m_{tp1c})|/m_{tp1c} \\ \Delta_{tp12}(m) &= |(m_{tp2} - m_{tp1})|/m_{tp1} \\ \Delta_{tp23}(m) &= |(m_{tp3} - m_{tp2})|/m_{tp2} \\ \Delta_{tp13}(m) &= |(m_{tp3} - m_{tp1})|/m_{tp1} \end{aligned} \tag{5}$$

where m denotes the mean value of the considered index along the fibers of a given connection, and the subscript c denotes the control group. Normality test (Kolmogorov-Smirnov) revealed that the values were normally distributed enabling the use of parametric statistics. Accordingly, the unpaired t-test with $p < 0.05$ was performed to establish the significant differences between $\Delta_{tp12c}(m)$ and $\Delta_{tp12}(m)$. With the purpose to further characterize the MAP-based indices, Spearman correlation with GFA was performed. In addition, for each patient, the z-score of the mean absolute changes of each index and connection with respect to the same measurement on the control group was calculated in order to highlight and visually render in an intuitive way the distance between each patient and the control group as well as individual changes over time. Finally, the predictive value of each metric was assessed by a linear regression model where the motor outcome at six months after stroke ($tp3$) was the dependent variable and the mean values of each index for all the connections at $tp1$, age, stroke size, and NIHSS motor scores at $tp1$ and $tp2$ were the predictors. A backward selection process was used to select the optimal predictor model with $p = 0.05$ as significance threshold.

3 Results and Discussions

Reproducibility of index values in controls. In controls, reproducibility of the mean GFA, RTAP, D and PA values was observed as confirmed by t-test which showed no statistical significant differences between *tp1c* and *tp2c* ($p > 0.05$). The mean absolute GFA, RTAP, D, and PA changes calculated for all the motor connections between the two time points were: $GFA : 0.0248 \pm 0.0074$, $RTAP : 0.0290 \pm 0.0082$, $D : 0.0205 \pm 0.0047$, $PA : 0.0241 \pm 0.0072$ (mean $\pm$ SEM). Among connections, the largest variability was recorded for SC.

Comparison of absolute GFA, RTAP, D, and PA changes in patients and controls. Figure 1 illustrates the mean absolute percent changes of the different indices for patients and controls. For each index, absolute changes between *tp1* and *tp2* in patients' connections were significantly different from the absolute

changes between the same regions in controls between *tp1c* and *tp2c* ($0.01 \leq p \leq 0.05$). However, the thalamic intracallosal connection failed to reach significance in all conditions, and SC-CC did not reach significance for RTAP and D. As it is apparent from Figure 1, PA shows the highest sensitivity in differentiating the patients from the control group, outperforming GFA in the SMA-CC connection and having the same performance for the other considered ones. In particular, both are able to differentiate the groups for the M1 and SC intracallosal connections. RTAP and D also allow differentiating between the two groups for M1 and SMA, while they could not highlight differences for SC. However, RTAP and D provide a richer microstructural information with respect to GFA which only describes the level of anisotropy of restricted diffusion. In connections where RTAP and D are able to split patients and controls, MAP-based indices allow for a more accurate description of the microstructural changes in patients.

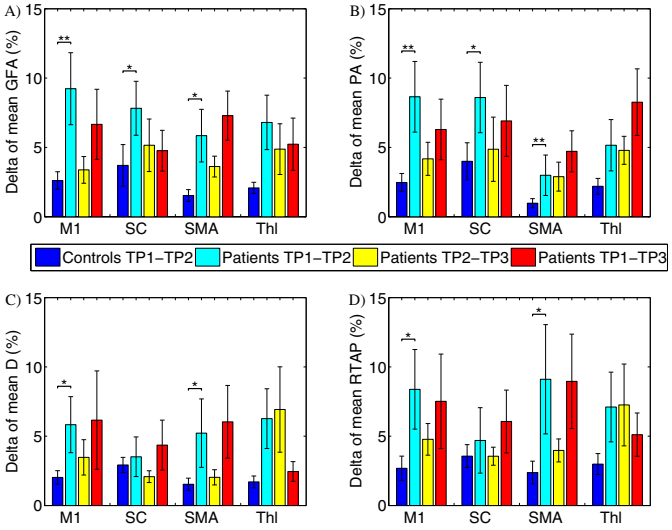

Fig. 1. Longitudinal changes in percent mean absolute values in controls and patients ($^*p < 0.05$, $^{**}p < 0.01$). (A) GFA; (B) PA; (C) D; (D) $RTAP$.

Correlations of each absolute descriptor changes with GFA. For both controls and patients, Spearman's correlation ρ showed a significant ($p < 0.05$) monotonic relationship between the mean absolute changes of each MAP-based index and GFA changes. The overall correlation among all the intracallosal connections was assessed, showing the following results: 1) RTAP: $\rho_{tp12c} = 0.48$, $\rho_{tp12} = 0.74$, $\rho_{tp23} = 0.38$, $\rho_{tp13} = 0.65$; 2) D: $\rho_{tp12c} = 0.43$, $\rho_{tp12} = 0.76$, $\rho_{tp23} = 0.37$, $\rho_{tp13} = 0.40$; and 3) PA: $\rho_{tp12c} = 0.51$, $\rho_{tp12} = 0.74$, $\rho_{tp23} = 0.40$, $\rho_{tp13} = 0.64$. In all cases results were significant with $p < 0.05$.

Longitudinal changes in patients. Figure 2 highlights the pattern of the longitudinal changes in the different connections for individual patients with respect

to the control group, that appeared to be patient-specific. The largest changes were observed in patients with the more severe motor deficit. The pattern is similar for the different indices providing evidence of the ability to capture the microstructural alterations due to white matter plasticity in the contralesional area. In particular, PA closely reproduces the pattern of GFA, while RTAP and D appear to be less sensitive especially for SC, coherently with the observation that for SC no significant difference between patients and controls could be detected by these two indices (see Figure 1). An increase in axon diameter is seen in patients over time. This could reveal axonal outgrowth and myelin increase due to plasticity as activated in the rehabilitation process [3], [11].

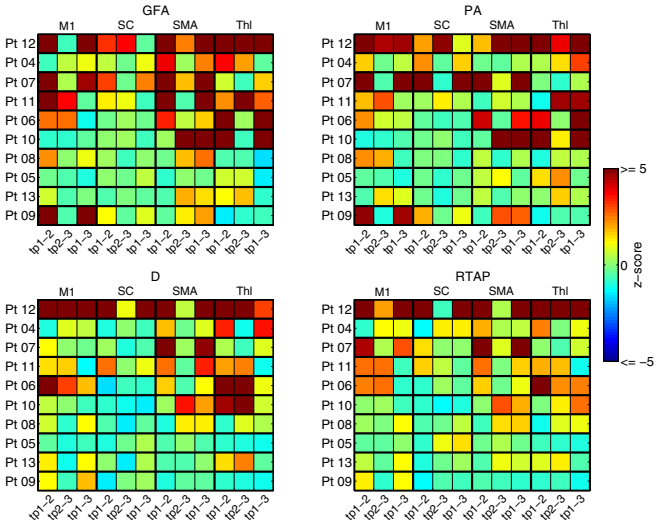

Fig. 2. Patients' individual profiles of mean absolute changes between *tp1* and *tp2* (first column), *tp2* and *tp3* (second column), and *tp1* and *tp3* (third column). Changes were compared to the corresponding controls' mean changes using z-scores. Patients are ordered according to the initial NIH Stroke Scale (NIHSS).

Prediction of clinical outcomes in patients for each index. In the patients' group, a linear regression model including only age and NIHSS at *tp1* and *tp2* gave low correlation as well as a model including only NIHSS at *tp1* and *tp2* ($R^2 = 0.691$; adjusted $R^2 = 0.652$). Conversely, for each index, the models including also its mean values across the different connections were able to predict the NIHSS at *tp3* with higher significance (Table 1). In particular, the best prediction model was obtained for D ($R^2 = 0.998$; adjusted $R^2 = 0.990$, $p = 0.008$). The relative importance for each predictor of the different optimal models was evaluated with the Fisher test and reported in Supplementary Materials. However, all models led to high significance, with adjusted $R^2 > 0.8$, confirming the importance of GFA and MAP-based indices for an early prediction of the patient clinical outcome.

Moreover, although GFA and PA are both anisotropy indices, PA has a higher prediction significance pointing at a stronger reliability of this new descriptor.

Table 1. Performance of each prediction model

Index	**Multiple R^2**	**Adjusted R^2**	***p***
GFA	0.970	0.932	0.004
RTAP	0.919	0.818	0.026
D	0.998	0.990	0.008
PA	0.991	0.973	0.004

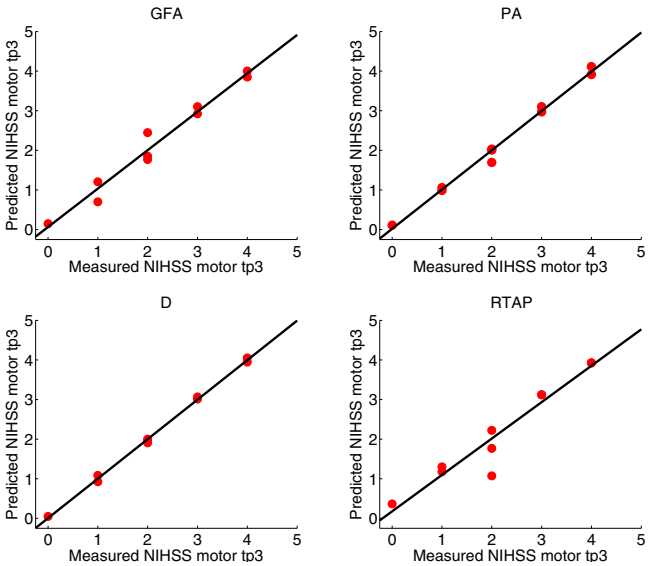

Fig. 3. Representation of the measured and predicted NIHSS at *tp3* using the models described above.

4 Conclusions

In this study, some evidence was provided on the suitability of the MAP-based indices RTAP, D, and PA as numerical biomarkers for stroke. Reproducibility was assessed by the test-retest method on the control group and longitudinal analysis on the patients group highlighted that contralesional structural changes after stroke could be well characterized and monitored by the newly proposed indices. The significant differences between controls and patients over multiple regions of interest lead the way to the application of RTAP, D, and PA as important descriptors for differentiating between the groups. Moreover, the performance of RTAP-, D-, and PA-based clinical regression models emphasized the suitability of these indices as early descriptors of patients' longitudinal changes and predictors of clinical outcomes.

References

1. Sotak, C.: The role of diffusion tensor imaging in the evaluation of ischemic brain injury a review. NMR in Biomedicine 15(7-8), 561–569 (2002)
2. Granziera, C., Daducci, A., Meskaldji, D., Roche, A., Maeder, P., Michel, P., Hadjikhani, N., Sorensen, A., Frackowiak, R., Thiran, J., Meuli, R., Krueger, G.: A new early and automated mri-based predictor of motor improvement after stroke. Neurology 79, 39–46 (2012)
3. Lin, Y., Daducci, A., Meskaldji, D., Thiran, J., Michel, P., Meuli, R., Krueger, G., Menegaz, G., Granziera, C.: Quantitative analysis of myelin and axonal remodeling in the uninjured motor network after stroke. Brain Connectivity (2014)
4. Ozarslan, E., Koay, C., Shepherd, T., Komlosh, M., Irfanoglu, M., Pierpaoli, C., Basser, P.: Mean apparent propagator (map) mri: A novel diffusion imaging method for mapping tissue microstructure. NeuroImage 78, 16–32 (2013)
5. Zucchelli, M., Descoteaux, M., Menegaz, G.: Human brain tissue microstructure characterization using 3D-SHORE on the HCP data. In: ISMRM, Toronto, Ontario, Canada (2015)
6. Ozarslan, E., Koay, C., Shepherd, T., Blackband, S., Basser, P.: Simple harmonic oscillator based reconstruction and estimation for three-dimensional q-space mri. Proc. Intl. Soc. Mag. Reson. Med. 17, 1396 (2009c)
7. Merlet, S., Deriche, R.: Continuous diffusion signal, {EAP} and {ODF} estimation via compressive sensing in diffusion {MRI}. Medical Image Analysis 17(5), 556–572 (2013)
8. Fick, R., Zucchelli, M., Girard, G., Descoteaux, M., Menegaz, G., Deriche, R.: Using 3D-SHORE and MAP-MRI to Obtain Both Tractography and Microstructural Constrast from a Clinical DMRI Acquisition. In: International Symposium on Biomedical Imaging: From Nano to Macro, Brooklyn, New York City, United States (2015)
9. Cheng, J., Jiang, T., Deriche, R.: Theoretical Analysis and Practical Insights on EAP Estimation via a Unified HARDI Framework. In: MICCAI Workshop on Computational Diffusion MRI (CDMRI), Toronto, Canada (2011)
10. Descoteaux, M., Angelino, E., Fitzgibbons, S., Deriche, R.: Regularized, fast, and robust analytical q-ball imaging. Magnetic Resonance in Medicine 58(3), 497–510 (2007)
11. Ueno, Y., Chopp, M., Zhang, L., Buller, B., Liu, Z., Lehman, N., Liu, X., Zhang, Y., Roberts, C., Zhang, Z.: Axonal outgrowth and dendritic plasticity in the cortical peri-infarct area after experimental stroke. Stroke 43(8), 2221–2228 (2012)